Report

Cell Reports

In Vivo DNA Re-replication Elicits Lethal Tissue Dysplasias

Graphical Abstract

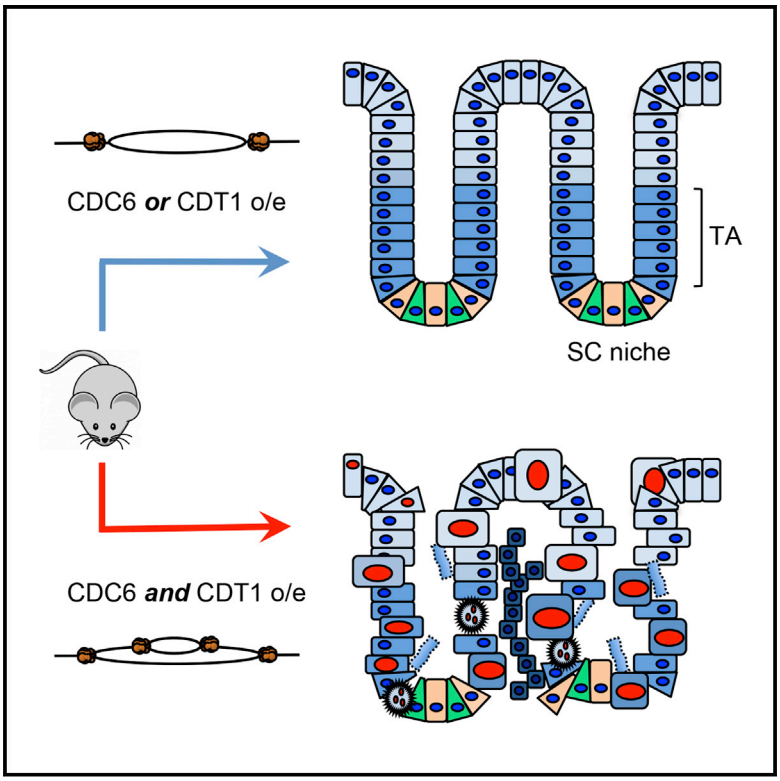

Authors

Sergio Muñoz, Sabela Búa, Sara Rodríguez-Acebes, Diego Megías, Sagrario Ortega, Alba de Martino, Juan Méndez

Correspondence

jmendez@cnio.es

In Brief

Muñoz et al. investigate the effects of deregulated DNA replication in vivo. The combined overexpression of CDC6 and CDT1, two key proteins that activate replication origins, resulted in aberrant origin reactivation, DNA overreplication, and lethal dysplasia in the intestine and other tissues.

Highlights

- Transgenic mouse strains allow Cdc6- and Cdt1-inducible overexpression
- Cdc6 and Cdt1 induce origin reactivation when expressed in combination
- DNA re-replication causes lethal dysplasias in intestinal epithelia and other tissues
- Levels of endogenous Cdc6 influence the sensitivity to Cdt1 deregulation in vivo

Muñoz et al., 2017, Cell Reports *19*, 928–938
May 2, 2017
http://dx.doi.org/10.1016/j.celrep.2017.04.032

CellPress

OPEN ACCESS
CellPress

Cell Reports
Report

In Vivo DNA Re-replication Elicits Lethal Tissue Dysplasias

Sergio Muñoz,[1,5] Sabela Búa,[1,5,6] Sara Rodríguez-Acebes,[1] Diego Megías,[2] Sagrario Ortega,[3] Alba de Martino,[4] and Juan Méndez[1,7,*]

[1]DNA Replication Group, Molecular Oncology Programme
[2]Confocal Microscopy Unit, Biotechnology Programme
[3]Transgenic Mice Unit, Biotechnology Programme
[4]Compared Pathology Unit, Biotechnology Programme
Spanish National Cancer Research Centre (CNIO), 3 Melchor Fernández Almagro, 28029 Madrid, Spain
[5]These authors contributed equally
[6]Present address: Institut Pasteur, 25 rue du Dr Roux, 75015 Paris, France
[7]Lead Contact
*Correspondence: jmendez@cnio.es
http://dx.doi.org/10.1016/j.celrep.2017.04.032

SUMMARY

Mammalian DNA replication origins are "licensed" by the loading of DNA helicases, a reaction that is mediated by CDC6 and CDT1 proteins. After initiation of DNA synthesis, CDC6 and CDT1 are inhibited to prevent origin reactivation and DNA overreplication before cell division. CDC6 and CDT1 are highly expressed in many types of cancer cells, but the impact of their deregulated expression had not been investigated in vivo. Here, we have generated mice strains that allow the conditional overexpression of both proteins. Adult mice were unharmed by the individual overexpression of either CDC6 or CDT1, but their combined deregulation led to DNA re-replication in progenitor cells and lethal tissue dysplasias. This study offers mechanistic insights into the necessary cooperation between CDC6 and CDT1 for facilitation of origin reactivation and describes the physiological consequences of DNA overreplication.

INTRODUCTION

Genomic stability relies on precise genome duplication. In mammalian cells, thousands of replication origins are "licensed" in the G1 phase by the binding of mini-chromosome maintenance (MCM) helicase complexes and become the starting points for bidirectional DNA synthesis in the S phase. After the G1/S transition, origins are not to be re-licensed or reactivated for the remainder of the cell cycle. In yeast, origin reactivation is a driver of gene amplification, copy number variation, and aberrant chromosome segregation (Green et al., 2010; Hanlon and Li, 2015). In mammalian cells, it causes chromosomal breaks and activation of the DNA damage response (Davidson et al., 2006; Neelsen et al., 2013).

The origin recognition complex (ORC) cooperates with CDC6 and CDT1 proteins to attract and engage the MCM helicase, forming pre-replicative complexes (pre-RCs) at the origins. CDC6 is an AAA+ ATPase, whereas CDT1 protein plays a chaperone function on MCM during the loading reaction (reviewed by Costa et al., 2013). Both CDC6 and CDT1 proteins are tightly regulated. CDC6 is targeted for degradation by ubiquitin ligases APC-Cdh1 in G1, CRL4-Cdt2 in S phase, and SCF-CycF in G2 (Méndez and Stillman, 2000; Petersen et al., 2000; Clijsters and Wolthuis, 2014; Walter et al., 2016). It is also translocated to the cytosol after G1/S (reviewed by Borlado and Méndez, 2008). In turn, CDT1 protein is targeted by ubiquitin ligases SCF-Skp2 and Cul4-Ddb1-Cdt2 (Nishitani et al., 2006) and inhibited by its interacting protein geminin in S and G2 (Wohlschlegel et al., 2000). CDC6 and CDT1 are also degraded as part of the cellular responses to restrict DNA replication upon DNA damage (Hu et al., 2004; Duursma and Agami, 2005).

These strict control mechanisms suggest that the cellular levels of CDC6 and CDT1 are critical for genomic integrity. Indeed, overexpression of Cdc6 and Cdt1 in pre-malignant cells promotes malignant behavior (Liontos et al., 2007), and both factors are overexpressed in several tumor types (reviewed by Petrakis et al., 2016). Transgenic mice expressing Cdt1 in thymocytes are prone to lymphoblastic lymphomas (Seo et al., 2005), and transgenic mice expressing Cdc6 in the skin are prone to papillomas (Búa et al., 2015). In p53 mutant cancer cells that proliferate despite expressing CDK inhibitor p21, genomic instability has been linked to the deregulation of CDC6 and CDT1 proteins (Galanos et al., 2016).

Despite these antecedents, the impact of systemic Cdc6 and Cdt1 deregulation in mammalian organisms had not been addressed. Here, we describe genetically modified mice strains in which Cdc6 and Cdt1 can be overexpressed during embryonic development or in adult tissues. Our results demonstrate the necessary cooperation between both proteins to induce origin re-licensing and re-firing in primary cells and show the lethal consequences of DNA re-replication in vivo.

RESULTS

Mouse Models with Inducible Cdc6 and/or Cdt1 Expression

Transgenic mouse embryonic stem cells (ESCs) were generated to allow the inducible expression of CDC6 and CDT1 proteins. A single copy of hemagglutinin (HA)-tagged Cdc6 cDNA, or FLAG-tagged Cdt1 cDNA, was inserted at the collagen 1 A1 (Col1A1) locus under the control of a tetracycline-responsive element. The M2 reverse tetracycline transactivator (M2-rtTA) is expressed from the Rosa26 locus, allowing tetracycline-inducible expression of the transgene (Figures 1A and 1B). The modified ESCs were used to generate HA-Cdc6 and Cdt1-FLAG transgenic mice, which were crossbred to generate a strain carrying both HA-Cdc6 and Cdt1-FLAG alleles in the Col1A1 loci. The three strains (from here on, TetO-Cdc6, TetO-Cdt1, and TetO-Cdc6+Cdt1) were viable and undistinguishable from wild-type (WT) mice in the absence of doxycycline (dox), the tetracycline derivative used to induce transgene expression.

The efficiency of Cdc6 and Cdt1 overexpression was confirmed in mouse embryonic fibroblasts (MEFs). Upon incubation with dox, HA-CDC6 and CDT1-FLAG proteins were expressed at approximately 10-fold higher levels than endogenous proteins (Figure 1C). This overexpression is within the 5- to 20-fold range observed in cancer cells (Tatsumi et al., 2006). Expression leakiness was ruled out by immunodetection of overexpressed proteins with antibodies that recognize the HA and FLAG epitopes and by comparisons of protein levels between WT and untreated TetO-Cdc6 and TetO-Cdt1 MEFs (Figures 1C and S1).

Transgenic HA-CDC6 and CDT1-FLAG proteins fluctuated in the cell cycle as their endogenous counterparts. HA-CDC6 levels dropped in G1, whereas CDT1-FLAG was less abundant in S phase, as expected (Figure S1B). Upon biochemical fractionation, both proteins were found in soluble and chromatin-bound forms, with higher levels of soluble CDC6 in S and G2/M (Figure S1B). HA-CDC6 and CDT1-FLAG proteins were degraded when cells were driven to quiescence and reaccumulated upon cell cycle re-entry (Figure S1C). Finally, both exogenous proteins were partially degraded in cells irradiated with UV (Figure S1D). These results indicate that exogenous HA-CDC6 and CDT1-FLAG proteins are subject to the regulatory mechanisms that control their endogenous counterparts.

Increased MCM Loading and Origin Activity after Cdc6 Overexpression

To test how Cdc6 and/or Cdt1 overexpression affected pre-RC formation in MEFs, the amount of MCM proteins on chromatin was estimated after biochemical fractionation. A 2-fold increase in chromatin-bound MCM was detected after the overexpression of Cdc6, but not Cdt1 (Figure 1D). Immunofluorescence (IF) intensity of chromatin-bound MCM3 increased only after Cdc6 overexpression (Figure 1E). The levels of geminin or other origin-activating proteins were not affected (Figure S1E). We conclude from these results that CDC6 is limiting for origin licensing in primary MEFs.

To evaluate the functional consequences of the increase in MCM chromatin association, the frequency of origin firing was estimated using stretched DNA fibers. Cdc6-overexpressing MEFs showed shorter inter-origin distances (median IOD 79.0 Kb) than control cells (median IOD 149 Kb; Figure 1F). These changes reflect an increase in origin activity, as IOD is inversely proportional to the frequency of origin firing. The same effect was observed in MEFs expressing Cdc6 and Cdt1, but not when Cdt1 was expressed individually. Increased origin activity can result in fork slowdown (Zhong et al., 2013). Upon Cdc6 overexpression, the median fork rate (FR) was reduced (“from 1.4 to 0.74 Kb/min; Figure 1G). This effect was not observed in Cdt1-overexpressing MEFs, except when expressed simultaneously to Cdc6. These results confirm the functionality of the “extra” pre-RCs formed after Cdc6 overexpression.

Combined Deregulation of Cdc6 and Cdt1 Triggers Origin Re-firing

In cancer cell lines, overexpression of Cdc6 or Cdt1 is sufficient to induce partial DNA re-replication (Vaziri et al., 2003). In primary MEF cultures, a population of tetraploid cells frequently coexists with a majority of diploid cells. Despite this fact, individual overexpression of Cdc6 or Cdt1 did neither affect their DNA content nor their ability to incorporate 5′-Bromo-2′-deoxyuridine (BrdU) (Figure 2A). When Cdc6 and Cdt1 were expressed simultaneously, a population of BrdU-negative cells accumulated with DNA content between 2C and 4C (Figure 2A, dashed gates). This population likely corresponds to originally diploid cells that underwent partial DNA re-replication, and its abundance increased by >5-fold upon Cdc6 and Cdt1 overexpression. This effect was separate from DNA endoreduplication after mitotic failure, which would result in tetraploid cells. An analysis of tetraploidy in multiple MEF isolates revealed no changes after dox treatment (Figure S1F). Cell proliferation was slowed down, but not arrested (Figure S1G).

The stretched DNA fiber assay was used to confirm the existence of origin re-firing. Cells were sequentially labeled with 5-Chloro-2′-deoxyuridine (CldU) for 2 hr (detected with red fluorescence) and 5-Iodo-2′-deoxyuridine (IdU) for 30 min (detected with green fluorescence). In this setting, origins that fired during the CldU pulse and re-fired during the IdU one would be identified as short yellow (green+red) signals embedded in longer red tracks. In agreement with the DNA content profiles, an increase in origin re-firing was found after the combined deregulation of Cdc6 and Cdt1 (Figure 2B). Whereas these events are likely to take place in S phase, we cannot rule out that some origins are reactivated in G2, as described for cancer cells after geminin ablation (Klotz-Noack et al., 2012). In this regard, TetO−Cdc6+Cdt1 MEFs positive for 5-Ethynyl-2′-deoxyuridine (EdU) incorporation that displayed a G2 pattern of phosphorylated H3 (pH3) could be identified (Figure S2A).

Origin re-firing has been linked to DNA damage (Davidson et al., 2006; Neelsen et al., 2013). Consistent with this notion, DNA damage marker γH2AX was elevated in TetO−Cdc6+Cdt1 MEFs after dox treatment (Figures 2C and S2B). The presence of double-strand breaks (DSBs) was confirmed by the detection of nuclear foci positive for γH2AX and 53BP1 (Figure S2C). The majority of γH2AX-positive cells had 2C or >2C DNA content, as expected for DNA damage caused by re-replication (Figure S2D). p53 was also activated in response to DNA damage (Figure 2C). Inhibition of CDK1 by phosphorylation could account for the slower cell proliferation (Figure S1G). Indeed, pH3

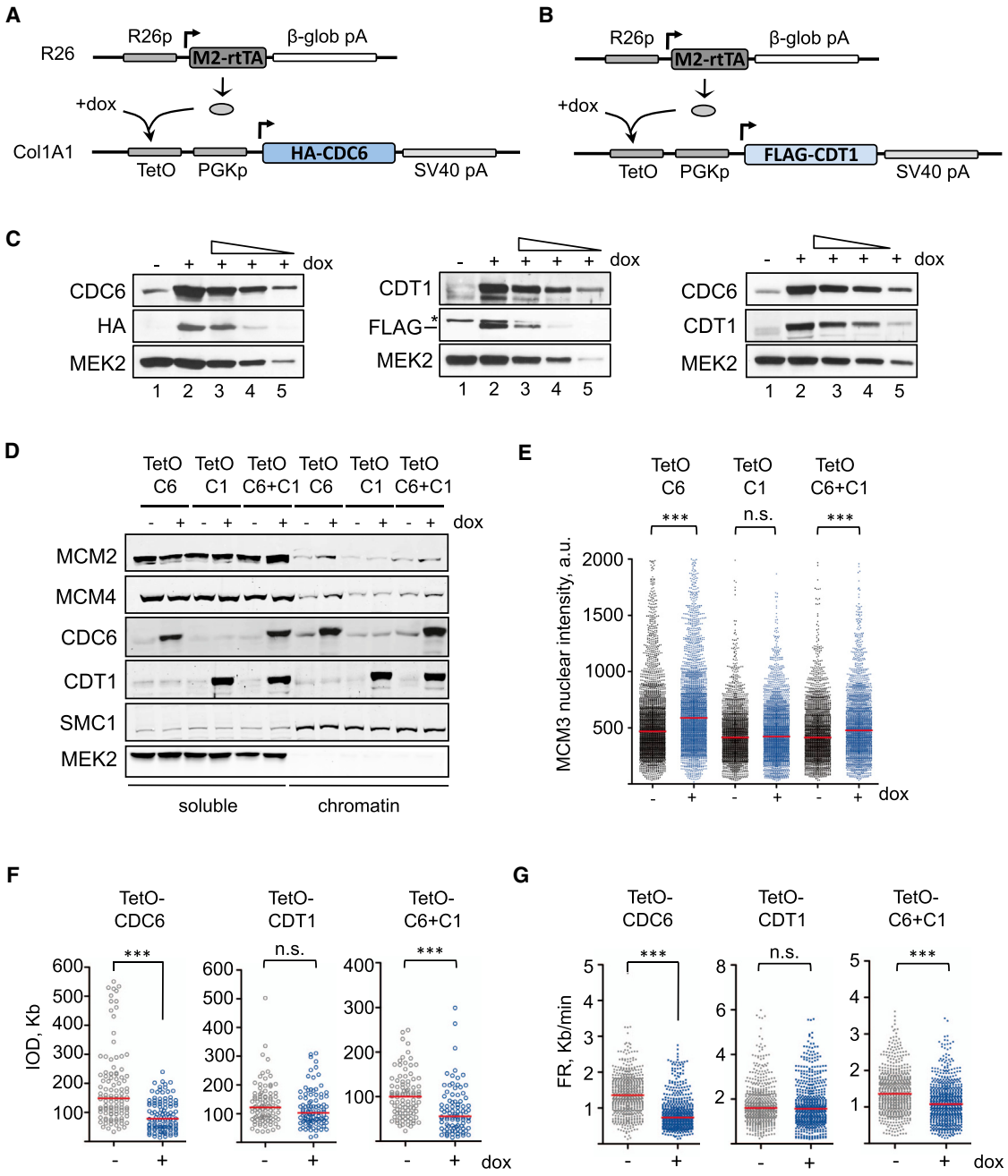

Figure 1. CDC6 Is a Limiting Factor for Pre-RC Formation

(A) Schematic of the TetO–Cdc6 genetic design.

(B) Schematic of the TetO–Cdt1 genetic design.

(C) Levels of CDC6 and CDT1 proteins in MEFs derived from TetO–Cdc6 (left), TetO–Cdt1 (middle), and TetO–Cdc6+Cdt1 mice. Endogenous levels are shown in lane 1. Lane 2 shows cells treated with 1 μg/mL dox for 24 hr. Lanes 3–5 show 50%, 25%, and 10% of the extract loaded in lane 2. HA and FLAG detect exogenously expressed CDC6 and CDT1, respectively. The asterisk marks a non-specific cross-reaction. MEK2 levels, loading control.

(D) Immunoblots in soluble and chromatin-enriched fractions of TetO–Cdc6 (C6), TetO–Cdt1 (C1), and TetO–Cdc6+Cdt1 (C6+C1) MEFs. MEK2 and SMC1, fractionation controls. Protein signal was detected in an Odyssey imaging system (LI-COR Biosciences).

(E) High-throughput acquisition of fluorescence intensity corresponding to chromatin-bound MCM3 protein in the indicated MEFs. A representative result from three experiments (>900 nuclei/condition) is shown. Kruskal-Wallis test was followed by Dunn's post-test; ***$p < 0.001$; n.s., not significant.

(F) Inter-origin distance (IOD) in the indicated MEFs. Data from two experiments are pooled (n = 88–106 measurements/condition).

(G) Fork rate (FR) values in the MEFs used in (F). Data from two separate experiments are pooled (n = 584–716 measurements/condition).

In (F) and (G), Mann-Whitney test was applied; ***$p < 0.001$. See also Figure S1.

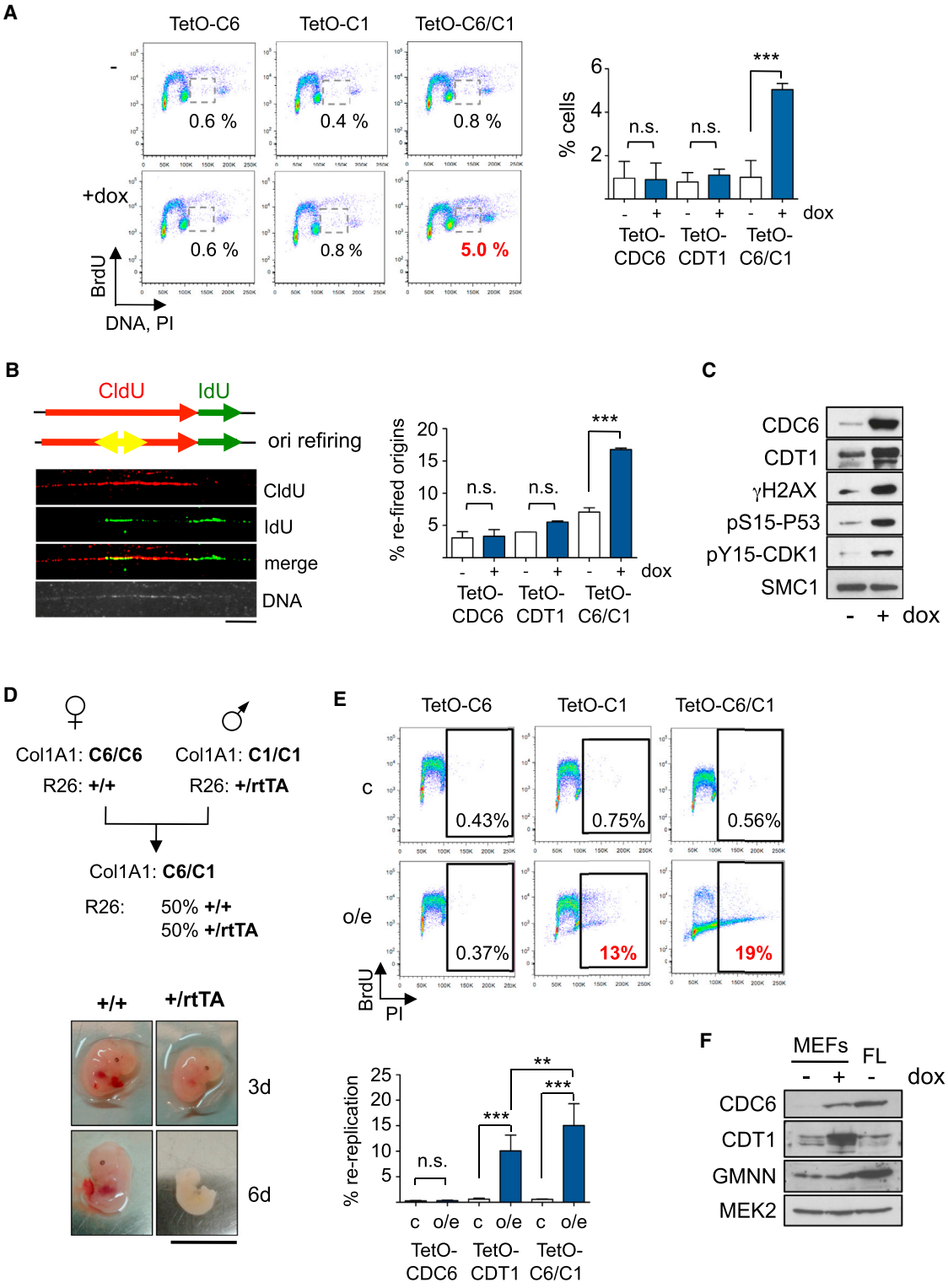

Figure 2. Cdc6 and Cdt1 Deregulation Triggers Re-replication

(A) Flow cytometry plots showing BrdU incorporation versus DNA content in the indicated MEFs with or without dox treatment. Dashed gates indicate BrdU-negative cells with DNA content between 2C and 4C. The histogram shows the percentage of cells within this gate (mean value and SD; n = 3 assays). ***$p < 0.001$; n.s., not significant in one-way ANOVA and Bonferroni's post-test.

(legend continued on next page)

patterns revealed an accumulation of cells in G2 and a decrease of cells in mitosis (Figure S2E). A 2-fold increase in apoptotic cells was also detected (Figure S2F). We conclude that the combined overexpression of Cdc6 and Cdt1 in primary MEFs induces origin re-firing, DNA overreplication, and DSBs, slowing down cell proliferation and increasing apoptosis.

Cdc6 and Cdt1 Deregulation Impairs Embryonic Development

We next studied the effects of deregulated Cdc6 and/or Cdt1 expression in embryonic tissues. A mating strategy was designed in which all embryos carried transgenic Cdc6 and Cdt1 but only 50% of them expressed rtTA, providing experimental and control embryos in the same litter (Figure 2D). When dox was added to the diet of pregnant females for 3 days in mid-gestation (embryonic day 10.5 [E10.5]–E13.5), half of the embryos were normal whereas the rest were smaller and pale. When dox was administered for 6 days (E6.5–E13.5), 50% of the embryos underwent regression (Figure 2D, bottom images). DNA replication was monitored in fetal liver cells pulse labeled with BrdU ex vivo. Normal embryos displayed no alterations in DNA content and BrdU incorporation, whereas up to 19% of the liver cells from underdeveloped embryos had >2C DNA content (Figure 2E). Molecular genotyping and immunoblots confirmed that all embryos undergoing re-replication were Cdc6+Cdt1 overexpressors (Figure S3). Similar experiments were conducted in the TetO−Cdc6 and TetO−Cdt1 strains. Cdc6 deregulation did neither affect embryonic development nor caused DNA re-replication in fetal liver cells. Interestingly, Cdt1 deregulation led to significant levels of DNA re-replication and embryonic regression (Figures 2E and S3). This result could be explained because fetal liver cells express high levels of endogenous CDC6 (even higher than dox-treated MEFs; Figure 2F). Of note, fetal liver cells also displayed high levels of GMN, the CDT1 inhibitor.

Cdc6 and Cdt1 Deregulation Causes Lethal Dysplasias in Adult Mice

To evaluate the impact of Cdc6 and Cdt1 deregulation in adult tissues, cohorts of TetO−Cdc6, TetO−Cdt1, and TetO−Cdc6+Cdt1 young mice were fed with dox-supplemented diet for 1 month. Control mice remained asymptomatic independently of their genotype. In the presence of dox, TetO−Cdc6 and TetO−Cdt1 mice did not display any visible phenotype, whereas TetO−Cdc6+Cdt1 mice suffered a significant weight loss and other signs of morbidity. Their mean survival time was less than 2 weeks (Figures 3A and 3B). Cdc6 and Cdt1 mRNA overexpression was confirmed in multiple tissues of TetO−Cdc6+Cdt1 mice (Figure 3C).

The rapid health deterioration of TetO−Cdc6+Cdt1 mice correlated with severe alterations in the gastrointestinal (GI) tract. The stomach showed gland disorganization and dysplasia. The crypt structures of the intestinal epithelium displayed mucosal atrophy, shortened villi, loss of goblet and Paneth cells, and some were filled with inflammatory cells and cellular debris (Figures 3D and S4A). Intestinal dysplasia impairs water and nutrient absorption, explaining the weight loss and morbidity. The GI tract of TetO−Cdt1 mice displayed related phenotypes in focal areas but not severe enough to cause morbidity (Figure S4A).

Outside the GI tract, histology alterations were found in the bone marrow (BM), spleen, and thymus of dox-treated TetO−Cdc6+Cdt1 mice (Figure S4B). The BM displayed moderate aplasia, lower presence of mature cells, nuclei with abnormal chromatin patterns, and increased apoptosis. The spleen showed activation of germinal centers and a high frequency of immature cells in the red pulp. The thymus of dox-treated TetO−Cdc6+Cdt1 mice showed severe cortical atrophy and was practically ablated in some individuals.

DNA Re-replication and DNA Damage in Intestinal Cells

The inner lining of the intestine is a rapidly renewing tissue. Because deregulation of Cdc6 and Cdt1 induced severe histological alterations, we tested whether DNA re-replication could be detected in cells isolated from this tissue. The percentage of intestinal cells with >2C DNA content was increased only in TetO−Cdc6+Cdt1 mice treated with dox (Figure 3E). In an alternative approach, the median DNA content of colon crypt cells was monitored in vivo using confocal microscopy. Higher DNA content was observed in the crypt cells of dox-treated TetO−Cdc6+Cdt1 mice, which must be caused by partial DNA re-replication (Figure 3F).

Origin re-firing and DNA re-replication induced DNA damage in vivo, as indicated by the elevated percentage of γH2AX-positive cells in and around the crypt structures of the colon (Figure 3G) or the stomach (Figure S5A) in dox-treated TetO−Cdc6+Cdt1 mice. Cells with >2C DNA content and DNA damage were also found in the BM (Figures S5B and S5C). Lower but detectable re-replication was observed in the BM of TetO−Cdt1 mice, which might be explained by high levels of endogenous Cdc6 expression (Wu et al., 2009; http://biogps.org/#goto=genereport&id=23834).

Activation of the DNA Damage Response and Increased Apoptosis

The cellular phenotypes caused by Cdc6 and Cdt1 deregulation in the intestine were analyzed by immunohistochemistry (IHC) using markers for proliferation (Ki67), cell cycle position (pH3),

(B) Origin re-firing event visualized in DNA fibers. The bar represents 10 μm. Histogram shows the percentage (mean and SD) of re-firing events relative to the total number of green tracks in the indicated MEFs (n = 2 assays/condition; 488–532 green track measurements/condition in each assay). ***p < 0.001. n.s., not significant in one-way Anova and Bonferroni's post-test.

(C) Immunoblots of the indicated proteins in TetO−Cdc6+Cdt1 MEFs. SMC1, loading control.

(D) Schematic of genetic cross and representative images of E13.5 embryos following dox administration for 3 or 6 days. +/+, control; +/rtTA, Cdc6+Cdt1 overexpressor embryos. The bar represents 1 cm.

(E) Flow cytometry analysis of fetal liver cells. Gates show cells with re-replicated (>2C) DNA content. Histogram shows percentage (mean and SD) of cells with >2C DNA content in the indicated embryos. TetON−Cdc6: n = 2 control (c) and 6 overexpressors (o/e); TetON−Cdt1: n = 6 c and 6 o/e; TetON−Cdc6+Cdt1: n = 5 c and 10 o/e. ***p<0.001; **p<0.01; n.s., not significant in one-way Anova and Bonferroni's post-test.

(F) Endogenous levels of CDC6, CDT1, and GMN in fetal liver (FL) cells and TetO−Cdc6+Cdt1 MEFs grown without or with dox. MEK2 levels, loading control. See also Figures S2 and S3.

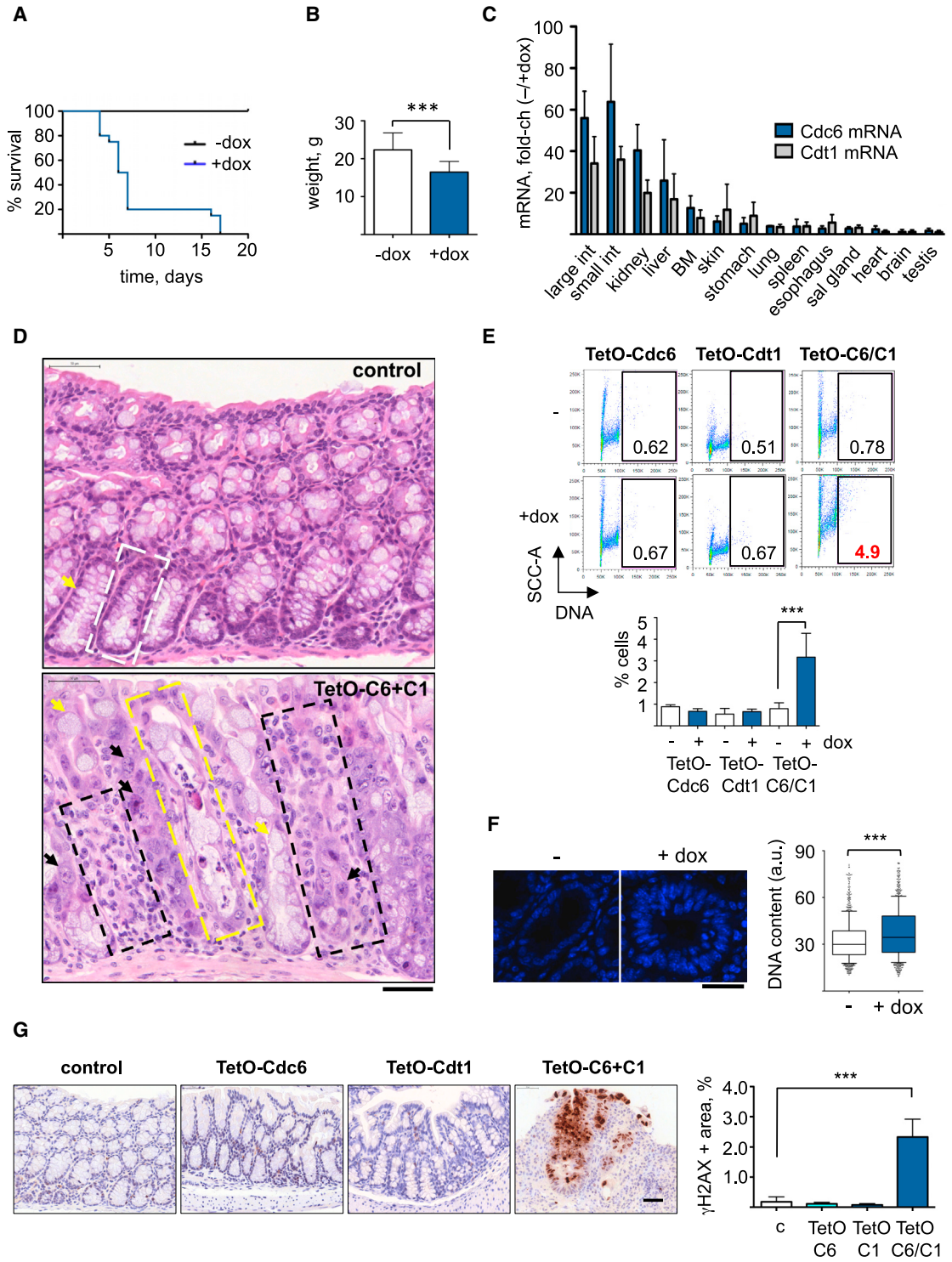

Figure 3. Cdc6 and Cdt1 Overexpression Is Lethal in Adult Mice

(A) Kaplan-Meier survival curves of TetO−Cdc6+Cdt1 mice (n = 16 control; 20 dox-treated).

(B) Weight (mean and SD) of control and dox-treated TetO−Cdc6+Cdt1 mice at the humane endpoint (n = 15 control; n = 16 dox treated). ***p < 0.001; Student's t test.

(C) Cdc6 and Cdt1 mRNA levels expressed as fold change (mean and SD) of dox-treated versus control TetO−Cdc6+Cdt1 mouse tissues; n = 4 mice/condition.

(legend continued on next page)

precursor cells (Sox9), DNA damage (p21), senescence (p16), and apoptosis (caspase 3). Ki67-positive cells were mainly located in the crypts in control mice and the remaining crypt-like structures in dox-treated mice and represent approximately 7% of the tissue area (Figure 4A). The number of precursor cells at the crypts was reduced upon Cdc6 and Cdt1 overexpression, as revealed by Sox9 staining (Figure 4B). The increase in p21 staining was consistent with the activation of a p53-mediated DNA damage response (Figure 4C). Specific pH3 staining patterns showed an increase in G2 cells, compatible with a checkpoint-induced G2/M arrest (Figures 4D and 4E). Regarding the outcome of cells that have accumulated DNA damage, staining with a senescence marker was virtually negative (Figure 4F), but a significant increase in apoptotic cells was observed (Figure 4G).

DISCUSSION

Alterations in origin activity generate replicative stress by different mechanisms (reviewed by Hills and Diffley, 2014; Muñoz and Méndez, 2017). Whereas the physiological consequences of DNA replication under conditions of limited origin licensing have been studied in mouse models hypomorphic for MCM, which are cancer prone and have hematopoietic defects (e.g., Shima et al., 2007; Pruitt et al., 2007; Alvarez et al., 2015), the loss of control over origin re-licensing and re-firing has not been addressed in vivo.

Previous work in cellular systems, mainly cancer cell lines, had identified control mechanisms that restrict the activity of pre-RC proteins to minimize re-replication. We report that these mechanisms can be overridden in vivo by the combined overexpression of Cdc6 and Cdt1, with lethal consequences for developing embryos and adult individuals. Whereas the possibility of other effects caused by protein overexpression cannot be completely ruled out, the fact that mice with individual overexpression of CDC6 or CDT1 displayed no phenotype argues that re-replication is the main cause of lethality in TetO−Cdc6+Cdt1 mice.

Not surprisingly, Cdc6 and Cdt1 deregulated expression affected highly proliferative cells and tissues. Fetal development was drastically stopped in mid-gestation. In adults, the effects were manifested after 1 or 2 weeks, when extensive disorganization of the GI tract correlated with weight loss and morbidity. Post-mortem analyses revealed alterations in several organs and striking dysplasias in the intestinal epithelium, which is subject to constant turnover to replenish dead cells. Epithelial regeneration is driven from "transit-amplifying" progenitors derived from stem cell niches located at the bottom of the intestinal crypts (reviewed by Barker, 2014). Upon Cdc6 and Cdt1 deregulation, transit-amplifying progenitors were particularly affected. Given that the epithelial renewal cycle takes 3–5 days in mice, the partial loss of these cells can explain the drastic tisular disorganization and intestinal failure.

Our study offers mechanistic insights into the regulation of mammalian replication origins (Figure 5A). Whereas both CDC6 and CDT1 proteins are required for origin licensing, CDC6 appears to be the limiting factor. This result is in agreement with recent in vivo data obtained in transgenic mice expressing Cdc6 in the skin: keratinocytes with high CDC6 levels displayed higher levels of MCM on chromatin (Búa et al., 2015). However, Cdc6 overexpression was not sufficient to induce origin re-firing because CDT1 is inhibited after the G1/S transition (Figure 5B). Consistent with the limiting role of CDC6, Cdt1 overexpression did neither increase origin licensing nor caused re-replication in primary cells (Figure 5C). Only when both factors were deregulated simultaneously, origins that had already been used could be re-licensed and re-fired, leading to DNA overreplication (Figure 5D).

The fact that deregulation of both Cdc6 and Cdt1 is necessary for origin re-licensing seems at odds with the fact that GMN downregulation or Cdt1 overexpression are sufficient to cause DNA re-replication in cancer cell lines (e.g., Vaziri et al., 2003; Melixetian et al., 2004). A likely explanation is that these cell lines express high levels of endogenous CDC6. In this study, we report that Cdt1 deregulation induced DNA re-replication in the fetal liver and the adult BM, two organs enriched in hematopoietic progenitors that express high levels of CDC6 (Wu et al., 2009). It is conceivable that rapidly dividing cells express higher levels of CDC6 to sustain faster proliferation. Beyond a threshold of CDC6 protein levels, deregulation of CDT1 would be sufficient to induce DNA overreplication (Figure 5E).

Cells with high levels of endogenous CDC6 and CDT1 may depend strictly on GMN to counteract the risk of re-replication. In this regard, genetic ablation of GMN in the hematopoietic system leads to a reduction of differentiated erythroid, myeloid, and lymphoid cells, and GMN-null leukocyte precursors undergo DNA re-replication (Shinnick et al., 2010; Karamitros et al., 2015). Another interesting case is ESCs that have adapted their cell cycle to allow rapid proliferation with short gap phases at the cost of undergoing replicative stress (Ahuja et al., 2016). ESCs express high levels of Cdc6 and Cdt1 (Fujii-Yamamoto et al., 2005; Ballabeni et al., 2011) and are highly dependent on GMN to avoid re-replication and apoptosis, but this dependency is alleviated after differentiation (Huang et al., 2015).

Finally, the fact that dox-treated TetO−Cdt1 mice are viable opens the possibility of unleashing CDT1 activity to trigger lethal re-replication in tumor cells with limited impact on the

(D) H&E stainings in control and dox-treated TetO−Cdc6+Cdt1 colon sections. The bar represents 50 μm. The white dashed box marks a crypt structure. Inflammatory infiltrates are shown in black dashed boxes. A crypt filled with cell debris is indicated by a yellow dashed box. Yellow arrows mark enlarged goblet cells. Black arrows mark cells with increased nuclear size and signs of stippled chromatin.
(E) Flow cytometry detection of side scatter area (SSC-A) versus DNA content in intestinal epithelial cells. Gates include cells with >2C DNA content. Histogram shows the percentage (mean and SD) of cells with >2C DNA content (n = 4 mice/strain and condition). ***$p < 0.001$ in one-way ANOVA and Bonferroni's post-test.
(F) DAPI-stained images of crypt cells from colon tissue of control and dox-treated TetO−Cdc6+Cdt1 mice. The bar represents 30 μm. Box plot shows integral intensity of DAPI staining (n = 3 mice/condition). More than 300 crypt cells were analyzed from four colon areas in each mouse. ***$p<0.001$ in Mann-Whitney test.
(G) γH2AX IHC staining in intestinal tissue of the indicated mice. The bar represents 50 μm. Histogram shows the percentage (mean and SD) of γH2AX-positive area. ***$p < 0.001$ in one-way ANOVA and Bonferroni's post-test.
See also Figures S4 and S5.

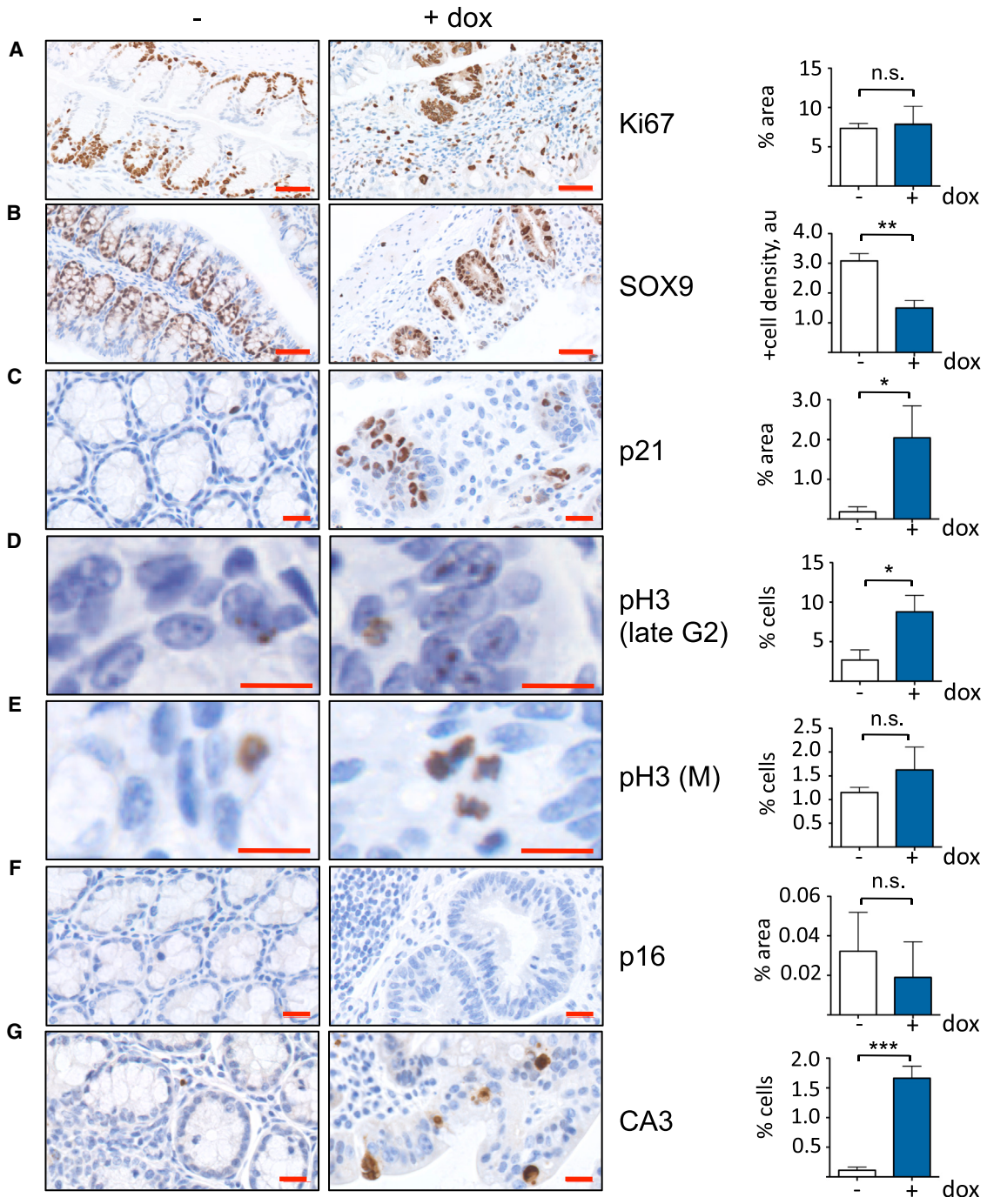

Figure 4. Cellular Responses to CDC6 and CDT1 Overexpression in the Intestine

Panels show representative images of IHC stainings in intestinal sections of control and dox-treated TetO–Cdc6+Cdt1 mice. The following antibodies were used: (A) Ki67; (B) Sox9; (C) p21; (D and E) pH3; (F) p16; and (G) activated caspase 3 (CA3). The bars represent 50 μm (A and B); 20 μm (C, F, and G); and 10 μM (D and E). Histograms show the quantification of positive signal in each case (mean and SD). CA3 and pH3 stainings were scored manually and are shown as % of positive cells (>1,200 total cells scored for pH3 from five different tissue areas per mouse; >1,400 total cells scored for CA3 from three different tissue areas per mouse). The rest were quantified automatically as % of positive area (n = 3 mice per condition). In the case of Sox9, automatic quantification also identified individual cells within the positive area, and the result is shown as density of positive cells. ***$p < 0.001$; **$p < 0.01$; *$p < 0.05$; n.s. = not significant in Student's t test.

surrounding tissues. Cellular studies have yielded promising results in this direction. GMN depletion is more toxic for cancer-derived cell lines than primary cells (Zhu and Depamphilis, 2009). Neddylation inhibitor MLN4924, used in clinical trials for leukemia, stabilizes CDT1 and kills tumor cells in part by inducing re-replication (Lin et al., 2010). The mouse strains characterized

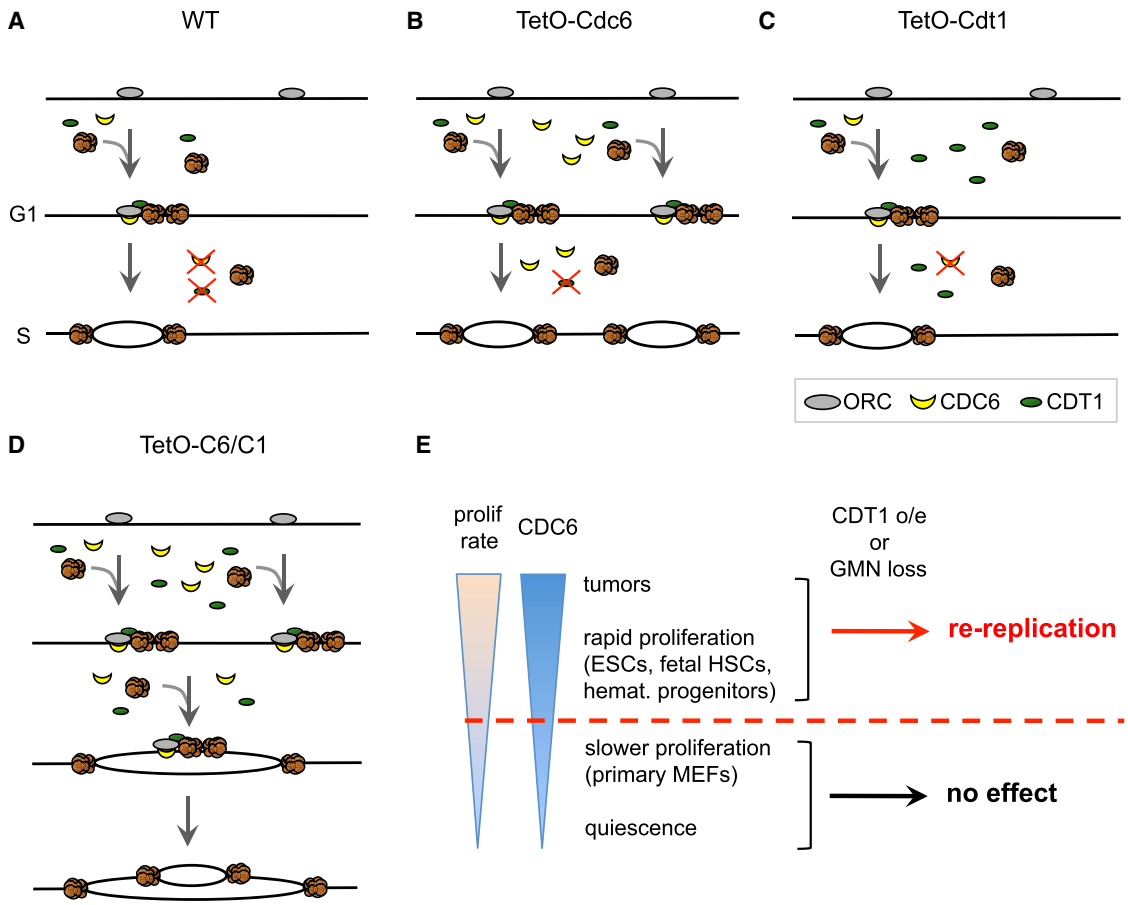

Figure 5. Necessary Cooperation of CDC6 and CDT1 for Origin Re-firing

(A) Hypothetical DNA region containing two potential origins marked by ORC. CDC6 protein limits pre-RC formation to only one origin. After G1/S, both CDC6 and CDT1 become limiting.

(B) Deregulated Cdc6 expression results in extra origin licensing and higher frequency of origin firing in S phase. CDT1 protein is still limiting after G1/S.

(C) Deregulated Cdt1 expression does not affect origin licensing because CDC6 is limiting in G1.

(D) Combined deregulation of Cdc6 and Cdt1 leads to origin re-licensing and re-replication.

(E) In primary cells, deregulation of Cdc6 and Cdt1 is necessary to induce re-replication. In contrast, cells with high proliferation rate and high levels of endogenous CDC6 are susceptible to re-replication induced by Cdt1 deregulation.

in our study reveal the marked cytotoxicity of DNA re-replication in vivo and may serve as useful models for pre-clinical studies.

EXPERIMENTAL PROCEDURES

TetO–Cdc6, TetO–Cdt1, and TetO–Cdc6+Cdt1 Mouse Strains

TetO–Cdc6 and TetO–Cdt1 mice strains were generated at the CNIO Transgenic Mice Unit, as described in Supplemental Experimental Procedures. Mice were housed at the CNIO Animal Facility in accordance with "Federation for Laboratory Animal Science Associations" guidelines. Young (2-month-old) mice of both sexes were used in all experiments. Animal procedures were approved by the Institutional Animal Care and Use Committee (IACUC) from Instituto de Salud Carlos III (Spain).

Molecular Genotyping and qRT-PCR

PCR genotyping at Rosa26 and Col1A1 loci was performed with Taq polymerase (Ecogen) on genomic DNA isolated from tail clips or embryonic tissue. Primer sequences are available upon request. For RT-PCR, tissues were disrupted in a bead-beating system (Precellys) and total RNA was isolated with Trizol (Invitrogen). Remaining genomic DNA was eliminated with DNaseI (Roche). 1 μg of total RNA was used for random-priming cDNA synthesis with SuperScript II (Invitrogen), and qPCR was performed using Power SYBR Green in an Applied Biosystems 7900HT Fast qRT-PCR machine. The $2^{\Delta\Delta Ct}$ method was used to quantify amplified fragments. Expression levels were normalized to GAPDH gene.

MEF Isolation and Procedures

TetO–Cdc6, TetO–Cdt1, and TetO–Cdc6+Cdt1 primary MEFs were derived from E12.5–14.5 embryos and cultured in DMEM with 10% fetal bovine serum (FBS) and antibiotics. Experiments were conducted at passage number $\leq$4. Except when indicated, dox was added for 24 hr. Whole-cell extracts were prepared by sonication in Laemmli buffer (Branson Digital Sonifier). Standard methods were used for SDS-PAGE and protein immunoblots. See Supplemental Experimental Procedures for a list of antibodies. When indicated, immunoblot signals were quantified in an Odyssey Imaging System (LI-COR Biosciences). For serum starvation and release assays, MEFs were kept at 100% confluency in DMEM-0.1% FBS for 72 hr and seeded at 50% confluency in DMEM-20% FBS. When indicated, MEFs were irradiated with 50 J/m^2 UV-C in a Hoefer Crosslinker 500. Biochemical fractionation was performed as described (Méndez and Stillman, 2000). For proliferation assays, aliquots of

50,000 cells were seeded in duplicates and counted at the indicated time points in a Neubauer hemocytometer. For BrdU incorporation and DNA content analyses by flow cytometry, see Supplemental Experimental Procedures.

Single-Molecule Analysis of DNA Replication

Stretched DNA fibers were prepared and analyzed as described (Mourón et al., 2013). A detailed protocol is provided in Supplemental Experimental Procedures.

IF Microscopy and High-Content Image Acquisition

Standard IF protocols were used (Supplemental Experimental Procedures). Images were acquired using a DM6000 B microscope or a SP2 AOBS Confocal Unit (Leica Microsystems). Definiens Developer XD software v.2.5 was used for γH2AX/53BP1 and pH3/EdU foci detection. When indicated, cells were cultured in μCLEAR bottom polylysine-treated 96-wells (Greiner Bio-One) and analyzed in an Opera High-Content Screening System with an APO 20×, 0.7 numerical aperture (NA) objective using Acapella software (PerkinElmer). To monitor DNA content in intestinal crypt cells, 3-μm colon sections were stained with DAPI. Images were acquired in a TCS-SP5 (AOBS) confocal microscope (Leica Microsystems) with a 20× HCX PL APO 0.7 NA dry objective. DAPI staining integral intensity was quantified using Definiens Developer XD software.

Histology and Immunohistochemistry

Tissues were fixed in 10% buffered formalin (Sigma) and embedded in paraffin using standard procedures. Three-micrometer sections were stained with H&E. Stainings were performed in an automatic Ventana Discovery XT platform (Roche). Tissue slides were digitalized using a Mirax scan or Axio Scan.Z1 (Carl Zeiss). CA3-positive and pH3-positive cells were scored manually. All other stainings were analyzed using AxioVision digital image software (Carl Zeiss). Areas of positive staining were normalized to the total tissue area.

SUPPLEMENTAL INFORMATION

Supplemental Information includes Supplemental Experimental Procedures and five figures and can be found with this article online at http://dx.doi.org/10.1016/j.celrep.2017.04.032.

AUTHOR CONTRIBUTIONS

S.M. and S.B. performed most experiments. S.R.-A. contributed to single-molecule analyses of DNA replication; D.M. contributed to confocal microscopy; S.O. participated in mouse strain generation; A.d.M. contributed histopathology analyses; J.M. designed and supervised the study; and S.M., S.B., and J.M. wrote the manuscript.

ACKNOWLEDGMENTS

We thank all members of the DNA Replication and Chromosome Dynamics Groups for discussions, S. Ruiz and I. Blanco for their help with mouse work, B. Urcelay for technical support, M. Udriste for assistance with IHC quantifications, U. Cronin and D. Martínez for assistance with flow cytometry experiments, M. Cañamero for the initial histopathology analyses, and O. Fernández-Capetillo for comments on the manuscript. Research was supported by MINECO grants BFU2013-49153-P, BFU2016-80402-R, and CSD2007-00015 to J.M. and MINECO predoctoral fellowships to S.M. and S.B.

Received: October 14, 2016
Revised: March 10, 2017
Accepted: April 12, 2017
Published: May 2, 2017

REFERENCES

Ahuja, A.K., Jodkowska, K., Teloni, F., Bizard, A.H., Zellweger, R., Herrador, R., Ortega, S., Hickson, I.D., Altmeyer, M., Mendez, J., and Lopes, M. (2016). A short G1 phase imposes constitutive replication stress and fork remodelling in mouse embryonic stem cells. Nat. Commun. *7*, 10660.

Alvarez, S., Díaz, M., Flach, J., Rodriguez-Acebes, S., López-Contreras, A.J., Martínez, D., Cañamero, M., Fernández-Capetillo, O., Isern, J., Passegué, E., and Méndez, J. (2015). Replication stress caused by low MCM expression limits fetal erythropoiesis and hematopoietic stem cell functionality. Nat. Commun. *6*, 8548.

Ballabeni, A., Park, I.H., Zhao, R., Wang, W., Lerou, P.H., Daley, G.Q., and Kirschner, M.W. (2011). Cell cycle adaptations of embryonic stem cells. Proc. Natl. Acad. Sci. USA *108*, 19252–19257.

Barker, N. (2014). Adult intestinal stem cells: critical drivers of epithelial homeostasis and regeneration. Nat. Rev. Mol. Cell Biol. *15*, 19–33.

Borlado, L.R., and Méndez, J. (2008). CDC6: from DNA replication to cell cycle checkpoints and oncogenesis. Carcinogenesis *29*, 237–243.

Búa, S., Sotiropoulou, P., Sgarlata, C., Borlado, L.R., Eguren, M., Domínguez, O., Ortega, S., Malumbres, M., Blanpain, C., and Méndez, J. (2015). Deregulated expression of Cdc6 in the skin facilitates papilloma formation and affects the hair growth cycle. Cell Cycle *14*, 3897–3907.

Clijsters, L., and Wolthuis, R. (2014). PIP-box-mediated degradation prohibits re-accumulation of Cdc6 during S phase. J. Cell Sci. *127*, 1336–1345.

Costa, A., Hood, I.V., and Berger, J.M. (2013). Mechanisms for initiating cellular DNA replication. Annu. Rev. Biochem. *82*, 25–54.

Davidson, I.F., Li, A., and Blow, J.J. (2006). Deregulated replication licensing causes DNA fragmentation consistent with head-to-tail fork collision. Mol. Cell *24*, 433–443.

Duursma, A., and Agami, R. (2005). p53-dependent regulation of Cdc6 protein stability controls cellular proliferation. Mol. Cell. Biol. *25*, 6937–6947.

Fujii-Yamamoto, H., Kim, J.M., Arai, K., and Masai, H. (2005). Cell cycle and developmental regulations of replication factors in mouse embryonic stem cells. J. Biol. Chem. *280*, 12976–12987.

Galanos, P., Vougas, K., Walter, D., Polyzos, A., Maya-Mendoza, A., Haagensen, E.J., Kokkalis, A., Roumelioti, F.M., Gagos, S., Tzetis, M., et al. (2016). Chronic p53-independent p21 expression causes genomic instability by deregulating replication licensing. Nat. Cell Biol. *18*, 777–789.

Green, B.M., Finn, K.J., and Li, J.J. (2010). Loss of DNA replication control is a potent inducer of gene amplification. Science *329*, 943–946.

Hanlon, S.L., and Li, J.J. (2015). Re-replication of a centromere induces chromosomal instability and aneuploidy. PLoS Genet. *11*, e1005039.

Hills, S.A., and Diffley, J.F. (2014). DNA replication and oncogene-induced replicative stress. Curr. Biol. *24*, R435–R444.

Hu, J., McCall, C.M., Ohta, T., and Xiong, Y. (2004). Targeted ubiquitination of CDT1 by the DDB1-CUL4A-ROC1 ligase in response to DNA damage. Nat. Cell Biol. *6*, 1003–1009.

Huang, Y.Y., Kaneko, K.J., Pan, H., and DePamphilis, M.L. (2015). Geminin is essential to prevent DNA re-replication-dependent apoptosis in pluripotent cells, but not in differentiated cells. Stem Cells *33*, 3239–3253.

Karamitros, D., Patmanidi, A.L., Kotantaki, P., Potocnik, A.J., Bähr-Ivacevic, T., Benes, V., Lygerou, Z., Kioussis, D., and Taraviras, S. (2015). Geminin deletion increases the number of fetal hematopoietic stem cells by affecting the expression of key transcription factors. Development *142*, 70–81.

Klotz-Noack, K., McIntosh, D., Schurch, N., Pratt, N., and Blow, J.J. (2012). Re-replication induced by geminin depletion occurs from G2 and is enhanced by checkpoint activation. J. Cell Sci. *125*, 2436–2445.

Lin, J.J., Milhollen, M.A., Smith, P.G., Narayanan, U., and Dutta, A. (2010). NEDD8-targeting drug MLN4924 elicits DNA rereplication by stabilizing Cdt1 in S phase, triggering checkpoint activation, apoptosis, and senescence in cancer cells. Cancer Res. *70*, 10310–10320.

Liontos, M., Koutsami, M., Sideridou, M., Evangelou, K., Kletsas, D., Levy, B., Kotsinas, A., Nahum, O., Zoumpourlis, V., Kouloukoussa, M., et al. (2007). Deregulated overexpression of hCdt1 and hCdc6 promotes malignant behavior. Cancer Res. *67*, 10899–10909.

Melixetian, M., Ballabeni, A., Masiero, L., Gasparini, P., Zamponi, R., Bartek, J., Lukas, J., and Helin, K. (2004). Loss of Geminin induces rereplication in the presence of functional p53. J. Cell Biol. *165*, 473–482.

Méndez, J., and Stillman, B. (2000). Chromatin association of human origin recognition complex, cdc6, and minichromosome maintenance proteins during the cell cycle: assembly of prereplication complexes in late mitosis. Mol. Cell. Biol. *20*, 8602–8612.

Mourón, S., Rodriguez-Acebes, S., Martínez-Jiménez, M.I., García-Gómez, S., Chocrón, S., Blanco, L., and Méndez, J. (2013). Repriming of DNA synthesis at stalled replication forks by human PrimPol. Nat. Struct. Mol. Biol. *20*, 1383–1389.

Muñoz, S., and Méndez, J. (2017). DNA replication stress: from molecular mechanisms to human disease. Chromosoma *126*, 1–15.

Neelsen, K.J., Zanini, I.M., Mijic, S., Herrador, R., Zellweger, R., Ray Chaudhuri, A., Creavin, K.D., Blow, J.J., and Lopes, M. (2013). Deregulated origin licensing leads to chromosomal breaks by rereplication of a gapped DNA template. Genes Dev. *27*, 2537–2542.

Nishitani, H., Sugimoto, N., Roukos, V., Nakanishi, Y., Saijo, M., Obuse, C., Tsurimoto, T., Nakayama, K.I., Nakayama, K., Fujita, M., et al. (2006). Two E3 ubiquitin ligases, SCF-Skp2 and DDB1-Cul4, target human Cdt1 for proteolysis. EMBO J. *25*, 1126–1136.

Petersen, B.O., Wagener, C., Marinoni, F., Kramer, E.R., Melixetian, M., Lazzerini Denchi, E., Gieffers, C., Matteucci, C., Peters, J.M., and Helin, K. (2000). Cell cycle- and cell growth-regulated proteolysis of mammalian CDC6 is dependent on APC-CDH1. Genes Dev. *14*, 2330–2343.

Petrakis, T.G., Komseli, E.S., Papaioannou, M., Vougas, K., Polyzos, A., Myrianthopoulos, V., Mikros, E., Trougakos, I.P., Thanos, D., Branzei, D., et al. (2016). Exploring and exploiting the systemic effects of deregulated replication licensing. Semin. Cancer Biol. *37-38*, 3–15.

Pruitt, S.C., Bailey, K.J., and Freeland, A. (2007). Reduced Mcm2 expression results in severe stem/progenitor cell deficiency and cancer. Stem Cells *25*, 3121–3132.

Seo, J., Chung, Y.S., Sharma, G.G., Moon, E., Burack, W.R., Pandita, T.K., and Choi, K. (2005). Cdt1 transgenic mice develop lymphoblastic lymphoma in the absence of p53. Oncogene *24*, 8176–8186.

Shima, N., Alcaraz, A., Liachko, I., Buske, T.R., Andrews, C.A., Munroe, R.J., Hartford, S.A., Tye, B.K., and Schimenti, J.C. (2007). A viable allele of Mcm4 causes chromosome instability and mammary adenocarcinomas in mice. Nat. Genet. *39*, 93–98.

Shinnick, K.M., Eklund, E.A., and McGarry, T.J. (2010). Geminin deletion from hematopoietic cells causes anemia and thrombocytosis in mice. J. Clin. Invest. *120*, 4303–4315.

Tatsumi, Y., Sugimoto, N., Yugawa, T., Narisawa-Saito, M., Kiyono, T., and Fujita, M. (2006). Deregulation of Cdt1 induces chromosomal damage without rereplication and leads to chromosomal instability. J. Cell Sci. *119*, 3128–3140.

Vaziri, C., Saxena, S., Jeon, Y., Lee, C., Murata, K., Machida, Y., Wagle, N., Hwang, D.S., and Dutta, A. (2003). A p53-dependent checkpoint pathway prevents rereplication. Mol. Cell *11*, 997–1008.

Walter, D., Hoffmann, S., Komseli, E.S., Rappsilber, J., Gorgoulis, V., and Sørensen, C.S. (2016). SCF(Cyclin F)-dependent degradation of CDC6 suppresses DNA re-replication. Nat. Commun. *7*, 10530.

Wohlschlegel, J.A., Dwyer, B.T., Dhar, S.K., Cvetic, C., Walter, J.C., and Dutta, A. (2000). Inhibition of eukaryotic DNA replication by geminin binding to Cdt1. Science *290*, 2309–2312.

Wu, C., Orozco, C., Boyer, J., Leglise, M., Goodale, J., Batalov, S., Hodge, C.L., Haase, J., Janes, J., Huss, J.W., 3rd, and Su, A.I. (2009). BioGPS: an extensible and customizable portal for querying and organizing gene annotation resources. Genome Biol. *10*, R130.

Zhong, Y., Nellimoottil, T., Peace, J.M., Knott, S.R., Villwock, S.K., Yee, J.M., Jancuska, J.M., Rege, S., Tecklenburg, M., Sclafani, R.A., et al. (2013). The level of origin firing inversely affects the rate of replication fork progression. J. Cell Biol. *201*, 373–383.

Zhu, W., and Depamphilis, M.L. (2009). Selective killing of cancer cells by suppression of geminin activity. Cancer Res. *69*, 4870–4877.